

Unsupervised Domain Adaptation for RF-based Gesture Recognition

Bin-Bin Zhang, Dongheng Zhang, Yadong Li, Yang Hu, and Yan Chen, *Senior Member, IEEE*

Abstract—Human gesture recognition with Radio Frequency (RF) signals has attained acclaim due to the omnipresence, privacy protection, and broad coverage nature of RF signals. These gesture recognition systems rely on neural networks trained with a large number of labeled data. However, the recognition model trained with data under certain conditions would suffer from significant performance degradation when applied in practical deployment, which limits the application of gesture recognition systems. In this paper, we propose an unsupervised domain adaptation framework for RF-based gesture recognition aiming to enhance the performance of the recognition model in new conditions by making effective use of the unlabeled data from new conditions. We first propose pseudo-labeling and consistency regularization to utilize unlabeled data for model training and eliminate the feature discrepancies in different domains. Then we propose a confidence constraint loss to enhance the effectiveness of pseudo-labeling, and design two corresponding data augmentation methods based on the characteristic of the RF signals to strengthen the performance of the consistency regularization, which can make the framework more effective and robust. Furthermore, we propose a cross-match loss to integrate the pseudo-labeling and consistency regularization, which makes the whole framework simple yet effective. Extensive experiments demonstrate that the proposed framework could achieve 4.35% and 2.25% accuracy improvement comparing with the state-of-the-art methods on public WiFi dataset and millimeter wave (mmWave) radar dataset, respectively.

Index Terms—Gesture Recognition, Cross Domain, Unsupervised Domain Adaptation, Radio Frequency.

I. INTRODUCTION

HUMAN gesture recognition plays an important role in human-computer interaction systems, which could be applied to smart home, smart driving and virtual reality, etc. Traditional approaches adopt cameras [1], [2], wearable devices and phones [4], [5] as the sensing front-end, which however suffer from inherent drawbacks including privacy leakage, inconvenience, and limited sensing range. To address this issue, significant efforts [12]–[15], [39]–[42], [67]–[73] have recently been made to achieve RF-based human gesture without letting the monitored subject carry any dedicated

This work was supported by National Natural Science Foundation of China under Grant 62201542, National Key Research and Development Program under Grant 2022YFC0869800, Key Research and Development Program of Anhui under Grant 2022h11020026, fellowship of China Postdoctoral Science Foundation under grant 2022M723069 and the Fundamental Research Funds for the Central Universities. (*Corresponding author: Yan Chen.*)

B. Zhang, D. Zhang, Y. Li, Y. Chen are with the School of Cyber Science and Technology, University of Science and Technology of China, Hefei 230026, China. (E-mail:{robin18, yadongli}@mail.ustc.edu.cn, {dongheng, eecyan}@ustc.edu.cn).

Y. Hu is with the School of Information Science and Technology, University of Science and Technology of China, Hefei 230026, China. (E-mail: eeyhu@ustc.edu.cn).

device. These systems recognize gestures by perceiving RF signals (e.g., WiFi or mmWave signals) variations caused by human gestures. However, the signals arriving at the receiver are not only determined by human gestures, but also significantly affected by the conditions of data collection. As a result, there exists huge discrepancies among data collected under one condition and another, which makes the recognition system suffer from severe performance degradation when deployed under new conditions.

Generally, RF signals are affected by three factors irrelevant to gesture: the environment for data collection, the subject which performs gesture, the location and orientation of the subject, which can be summarized using the term “domain”. The source domain data denotes the signals collected under specific conditions, which are adopted to train the recognition model. The signals collected under new conditions are referred as target domain data, which are obtained in practical deployment and unseen for the recognition model. With the data discrepancies between these two domains, the performance of existing human gesture systems are limited in real-world deployment.

To resolve this problem, existing methods have investigated new mathematical models to eliminate the effects of domain factors [16], [17], neural network architectures to extract domain-invariant features [18], [19], [46]. However, the performance enhancements by these investigations are still limited, which makes the problem still unresolved. To tackle this challenge, we have noted that all these methods optimize the system using the labeled source domain data in a supervised manner. Due to the lack of labels in target domain, the information in the target domain data are actually wasted.

In this paper, we propose an unsupervised domain adaptation framework for RF-based human gesture recognition to improve the performance on unlabeled target domain. The basic idea is to employ the pseudo-labeling and consistency regularization to make effective use of the unlabeled target domain data in an unsupervised manner. The pseudo-labeling can generate pseudo labels from unlabeled target domain data to train model, and the consistency regularization is to eliminate the feature discrepancies in different domains for enhancing the robustness of neural network. However, deploying the pseudo-labeling and consistency regularization is non-trivial and we face three challenges:

- Obtaining the pseudo labels of the unlabeled target domain data and utilizing them to training the model is an important process. However, the existing works [81], [82] show that incorrect pseudo labels are inevitable due to the limitation of the recognition model and the gap between

source domain and target domain, which leads to significant performance degradation of the model.

ii) Data augmentation methods are necessary to consistency regularization. However, unlike optical images, the semantic information in RF signals are usually not interpretable intuitively. The data augmentation methods including flipping and rotating for optical images would change the semantic information of the RF signals, which would be harmful to model training. Hence, we need to design effective data augmentation methods for RF signals.

iii) The proposed framework utilizes the unlabeled new domain data in an unsupervised manner. Computing and optimizing the two unsupervised losses (self-supervised loss and consistency regularization loss) would bring about the considerable computational burden, which greatly weakens the real-time performance of the system.

In this work, to attenuate the negative effects of incorrect pseudo labels on recognition model, we propose a confidence constraint loss to enhance the effectiveness of pseudo-labeling. To strengthen the performance of the consistency regularization, we design two corresponding data augmentation methods based on the characteristic of the RF signals. Moreover, we propose a cross-match loss integrating pseudo-labeling and consistency regularization to alleviate the computational burden.

The main contributions of our work are summarized as following:

(1) We propose an unsupervised domain adaptation framework for RF-based human gesture recognition, which can utilize the unlabeled target domain data to improve the performance of the recognition model.

(2) We propose a cross-match loss combining pseudo-labeling and consistency regularization, which could utilize the unlabeled target domain data to train in a self-supervised manner and eliminate the feature discrepancies in different domains.

(3) We propose a confidence constraint loss to enhance the effectiveness of pseudo-labeling, and design two corresponding data augmentation methods based on the characteristic of the RF signals to strengthen the performance of the consistency regularization, which can make the framework more effective and robust.

(4) We conduct comprehensive experiments on the two RF public datasets (i.e., Wi-Fi dataset and mmWave radar dataset). The proposed framework achieves state-of-the-art results, which demonstrates that our framework is effective and universal for different kinds of RF signals.

The rest of this paper is organized as follows. Section II introduces the related work. Section III formulates the problem. Section IV introduces the system overview, recognition model and the proposed unsupervised domain adaptation framework. Section V presents the experiments on the two RF signals, the performance of the cross domain evaluations and the ablation study. Section VI concludes this paper.

II. RELATED WORK

The proposed framework is mainly related to three techniques: *cross domain gesture recognition*, *unsupervised domain adaptation* and *semi-supervised learning*.

A. Cross Domain Gesture Recognition

Wireless human sensing techniques [65], [66], [74]–[76], [78] have drawn considerable attentions and made great progresses in recent years. Since human gesture recognition plays an important role in human-computer interaction, researchers have explored how to achieve gesture recognition with RF signals. There are many prior works focusing on cross domain gesture recognition to reduce data collection and labeling efforts to generalize the recognition model, which can be roughly divided into two categories: WiFi-based and mmWave-based methods.

Among the WiFi-based methods, WiAG [16] and Widar3.0 [17] construct mathematical models to derive domain-invariant features. CrossSense [18] proposes an offline trained ANN-based roaming model mapping features from one environment to another. EI [19] uses an adversarial training scheme together with several constraints to generalize the model to new environments and new subjects. For the mmWave-based models, Liu et al. [44] extract dynamic variation of gestures from mmWave signals and design a lightweight CNN to recognize gestures. MmASL [45] designs a multi-task deep neural network to achieve American sign language recognition. RadarNet [46] designs an efficient neural network and collects a large scale dataset to train a robust model. However, even though the above methods have achieved the decent performance, the progress is limited and costly. The main reason is that these methods can not make effective use of the information in the target domain data to adapt the recognition model due to lack of the labels. In this paper, we propose an unsupervised domain adaptation framework for RF gesture recognition to make effective use of the target domain data without labels, which can enhance the performance of the recognition model on the target domain.

B. Unsupervised Domain Adaptation

The Unsupervised Domain Adaptation (UDA) models assume that the source domain has sufficient labels, while the unlabeled target domain participates the model training in an unsupervised manner [55]. Several approaches are adopted to learn domain-invariant features through different metrics, e.g., Maximum Mean Discrepancy (MMD) [57], [58]. Contrastive Adaptation Network (CAN) [59] optimizes the metric for minimizing the domain discrepancy, which explicitly models the intra-class domain discrepancy and the inter-class domain discrepancy. Deep Adaption Network (DAN) [57] adapts the high-layer features with the multi-kernel MMD criterion. Adversarial discriminative domain adaptation (ADDA) [60] learns a discriminative representation using the source labels, and then, a separate encoding that maps the target data to the same space based on a domain-adversarial loss is used. General to Adapt (GTA) [61] introduces a symbiotic relation between the embedding network and the generative adversarial network. Some other methods aim to learn a feature extractor to extract the domain-invariant features, and maintain the representation consistency through minimizing the reconstruction error between domains. For example, Domain Adversarial Neural Network (DANN) [63] proposes a domain-adversarial

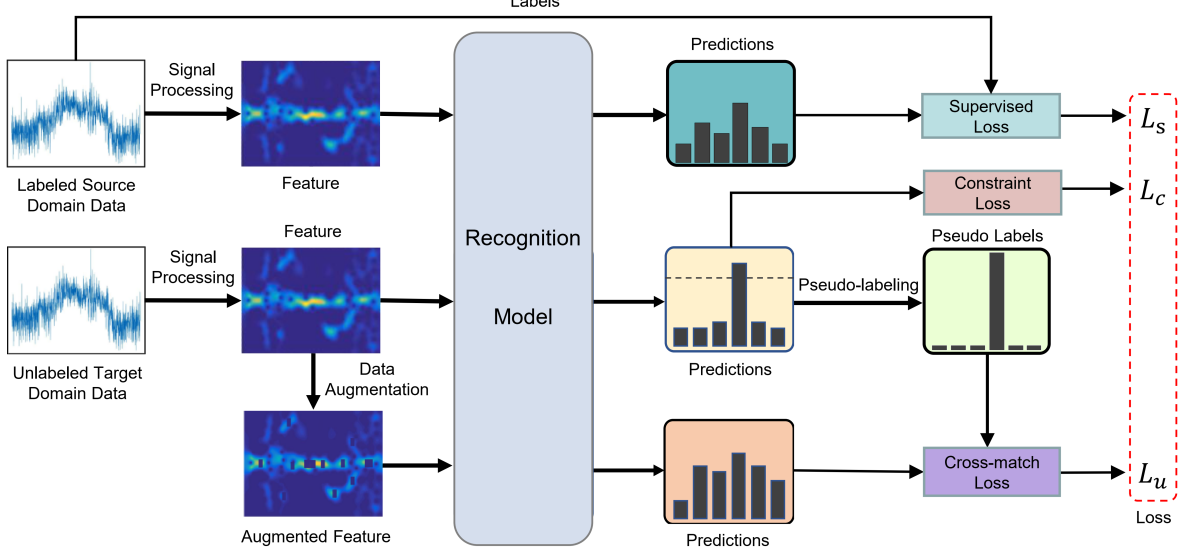


Fig. 1. Overview of the framework. We first augment the raw unlabeled target domain data to obtain the augmented data, then the labeled data and unlabeled data are simultaneously fed into the model to obtain three groups of predictions. After obtaining the pseudo labels from the predictions of raw unlabeled target domain data, we adopt the pseudo labels as the ground truth of the predictions of the augmented data and compute the cross-match loss L_u between them. Moreover, the supervised loss L_s between the predictions of the source domain feature and labels is computed for model training, and a confidence constraint loss L_c is adopted to enhance the effectiveness of pseudo-labeling. During training, the three losses are optimized simultaneously.

training method to promote the emergence of features that are discriminative for the main learning task on the source domain. Unsupervised Image-to-Image Translation (UNIT) [64] makes a shared-latent space assumption and proposes an unsupervised image-to-image translation framework based on Coupled GANs. Different from existing methods based on vision modality, our work focuses on how to design effective framework for RF-based gesture recognition systems.

C. Semi-Supervised Learning

Semi-supervised learning (SSL) [25], [27], [29], [47]–[49] leverages unlabeled data to improve the performance of models when limited labeled data is provided, which alleviates the expensive labeling process efficiently. Some recently proposed semi-supervised learning methods, such as MixMatch [48], FixMatch [27], and ReMixMatch [47] are based on augmentation viewpoints. MixMatch [48] uses low-entropy labels for data-augmented unlabeled instances and mixes labeled and unlabeled data for semi-supervised learning. FixMatch [27] generates pseudo labels using the model’s predictions on weakly augmented unlabeled images. ReMixMatch [47] uses a weakly-augmented example to generate an artificial label and enforce consistency against strongly-augmented examples. Semi-supervised domain adaptation has more information about some target labels compared with UDA, and some related works [50]–[54] have been proposed leveraging semi-supervised signals. Specifically, in [51], a minimax entropy approach is proposed that adversarially optimizes an adaptive few-shot model. In [52], the learning of opposite structures is unified whereby it consists of a generator and two classifiers trained with opposite forms of losses for a unified object. The design of the proposed framework is inspired by the principles

of SSL, while we focus on domain adaption for RF signals, which has not been considered in existing works.

III. PROBLEM FORMULATION

Given N source domain gesture data $\{\mathbf{X}_{s_i}, \mathbf{Y}_{s_i}\}_{i=1}^N$ with labels and a target domain gesture data \mathbf{X}_t without labels, the recognition model is trained using the source domain data and tested on the target domain. Especially, to enhance the performance of the recognition model on target domain, the recognition model is allowed to utilize the target domain data without the labels. However, the target domain data can not be directly utilized for training model due to lack of labels. Thus, the recognition model trained using only the source domain data suffers from the performance degradation when applied on the target domain.

To tackle the problem, an unsupervised domain adaptation framework is proposed to make effective use of the unlabeled target domain data to enhance the performance of the gesture recognition model on the target domain.

IV. METHODOLOGY

Existing gesture recognition systems capture RF data frames and feed data into neural network models after pre-processing. The proposed framework is built upon this pipeline which utilizes both labeled source domain data and unlabeled target domain data to optimize the neural network model as shown in Fig. 1. Specifically, we first generate pseudo labels for unlabeled target domain data with confidence control to utilize these data for model training. We then utilize consistency regularization to eliminate the feature discrepancies in different domains. Furthermore, we propose a cross-match loss combining the pseudo-labeling and consistency regularization, which makes the whole framework simple yet effective. Finally, we

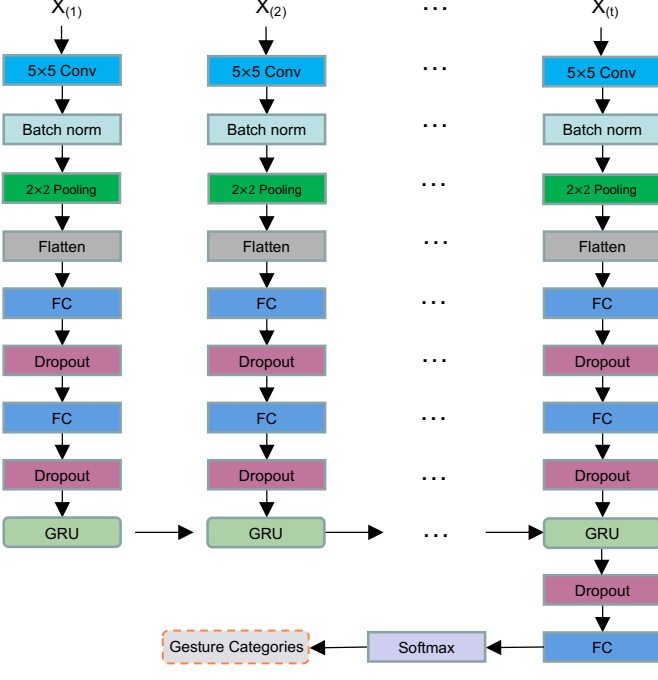


Fig. 2. Structure of gesture recognition model.

design a confidence constraint loss and two data augmentation methods based on the characteristic of RF signals to enhancing the performance of our framework. In the following, we will introduce our framework in detail.

A. Gesture Recognition Model

We adopt a neural network model combing Convolutional Neural Network (CNN) layers and Gated Recurrent Units (GRU) as the gesture recognition model as shown in Fig. 2. Specifically, the input data \mathbf{X} are first fed into 2D CNN layers, max-pooling layers and dropout layers for feature extraction. Then, the features are flattened and fed into fully-connected layers with ReLu activation to obtain higher level representation $\{\mathbf{U}_i\}_{i=1}^T$. Finally, $\{\mathbf{U}_i\}_{i=1}^T$ is fed into GRUs to furhter extract temporal information. The output of the neural network can be expressed as

$$\hat{\mathbf{Y}} = \mathbf{G}(\mathbf{X}; \theta), \quad (1)$$

where θ denotes the parameters of the recognition model \mathbf{G} , $\hat{\mathbf{Y}}$ denotes the output label of gesture category.

In conventional gesture recognition systems, researchers utilize the labeled source domain gesture data \mathbf{X}_s with label \mathbf{Y}_s to train the recognition model then deploy the model in practical systems. However, due to the data discrepancies among different domains, the model trained on source domain would suffer from significant performance degradation in target domain. To resolve this problem, in the paper, an unsupervised domain adaptation framework is proposed to enhance the performance of gesture recognition model by making effective use of the unlabeled target domain RF data.

B. Unsupervised Domain Adaptation Framework

1) *Input and Output*: The proposed framework utilizes both the labeled source domain data and unlabeled target domain data to train the recognition model. We first select B labeled data $\{\mathbf{x}_s, \mathbf{y}_s\}$ from the source domain gesture data pool $\{\mathbf{X}_s, \mathbf{Y}_s\}$ and μB unlabeled data \mathbf{x}_t from target domain gesture data pool \mathbf{X}_t , where B is the batch size of the labeled data at every iteration, μ is a hyper-parameter. Then we perform data augmentation on \mathbf{x}_t to obtain data \mathbf{x}_t^{aug} . The data augmentation operation is denoted by $\mathcal{A}(\cdot)$, which would be introduced in the following. After that, the source domain labeled data \mathbf{x}_s , unlabeled target domain data \mathbf{x}_t , and augmented version data \mathbf{x}_t^{aug} are concatenated as follows:

$$\begin{aligned} \mathbf{x}_t^{aug} &= \mathcal{A}(\mathbf{x}_t), \\ \mathbf{X} &= \mathbf{x}_s \oplus \mathbf{x}_t \oplus \mathbf{x}_t^{aug}, \end{aligned} \quad (2)$$

where \oplus denotes the concatenation operation of the matrix. After \mathbf{X} being fed into the recognition model, the predictions $\hat{\mathbf{Y}}$ can be obtained, which is composed of three parts as follows:

$$\hat{\mathbf{Y}} = \hat{\mathbf{y}}_s \oplus \hat{\mathbf{y}}_t \oplus \hat{\mathbf{y}}_t^{aug}, \quad (3)$$

where $\hat{\mathbf{y}}_s$ is the predictions of \mathbf{x}_s , $\hat{\mathbf{y}}_t$ represents the predictions of \mathbf{x}_t , and $\hat{\mathbf{y}}_t^{aug}$ denotes the predictions of \mathbf{x}_t^{aug} .

2) *Supervised Loss*: Due to the fact that $\hat{\mathbf{y}}_s$ have the labels \mathbf{y}_s , we can directly compute the cross-entropy loss between $\hat{\mathbf{y}}_s$ and \mathbf{y}_s as follows:

$$L_s = -\frac{1}{B} \sum_{i=1}^B \mathbf{y}_s^{(i)} \log(\hat{\mathbf{y}}_s^{(i)}). \quad (4)$$

By computing the supervised loss L_s , the source domain data $\{\mathbf{X}_s, \mathbf{Y}_s\}$ are utilized to train the recognition model. The supervised loss is the component of the objective function that is adopted to compute the gradients and update the parameters during the training. Moreover, due to the $\hat{\mathbf{y}}_t$ and $\hat{\mathbf{y}}_t^{aug}$ lacking of the labels, we adopt the pseudo-labeling and consistency regularization to make effective use of them in an unsupervised manner.

3) *Pseudo-labeling*: To make effective use of the unlabeled target domain data, we first utilize the pseudo-labeling to generate pseudo labels of target domain data. Specifically, with the output $\hat{\mathbf{y}}_t$, we adopt the largest prediction score which surpasses the threshold τ as the pseudo label, which can be expressed as:

$$\mathbf{y}_t^{p(j)} = \begin{cases} 1, & \hat{\mathbf{y}}_t^{(j)} \geq \tau, \\ 0, & \text{otherwise.} \end{cases} \quad j = 1, 2, \dots, C, \quad (5)$$

where C denotes the number of gesture classes. After obtaining the pseudo labels \mathbf{y}_t^p , the self-supervised loss L_{self} is computed as follows:

$$L_{self} = -\frac{1}{P} \sum_{i=1}^P \mathbf{y}_t^{p(i)} \cdot \log(\hat{\mathbf{y}}_t^{(i)}), \quad (6)$$

where P is the number of pseudo labels, $\hat{\mathbf{y}}_t$ denotes the predictions of the model on target domain. Different from traditional methods which directly optimize the loss L_{self} for

model training, in this paper, we propose a cross-match loss to combine the pseudo-labeling and consistency regularization in a simple way, which aims to decrease the computation cost.

4) *Consistency Regularization*: Apart from pseudo-labeling, we also propose consistency regularization to make effective use of the unlabeled target domain data for enhancing the robustness of neural network. The core of consistency regularization lies in the fact that the outputs of the model should be consistent when the input data is disturbed slightly if the model is well trained. The conventional methods randomly disturb the data \mathbf{x}_t to obtain the different version. However, [28] demonstrates that adopting the data augmentation methods to transform data \mathbf{x}_t could make the consistency regularization perform better. Since existing data augmentation methods for visual images can not be directly applied to RF signals, we propose two data augmentation methods: *Local Feature Erasing* and *Time Erasing* to enhance the performance of the consistency regularization. After transforming the original data \mathbf{x}_t into a different version \mathbf{x}_t^{aug} by using the data augmentation methods, the original data \mathbf{x}_t and the augmentation version \mathbf{x}_t^{aug} are fed into the recognition model to obtain the predictions $\hat{\mathbf{y}}_t$ and the predictions $\hat{\mathbf{y}}_t^{aug}$, respectively. The discrepancies between the predictions $\hat{\mathbf{y}}_t$ and $\hat{\mathbf{y}}_t^{aug}$ are measured using cross entropy, which are referred as the consistency regularization loss L_{reg} . The consistency regularization loss L_{reg} is computed as follows:

$$L_{reg} = -\frac{1}{P} \sum_{i=1}^P \hat{\mathbf{y}}_t^{(i)} \cdot \log(\hat{\mathbf{y}}_t^{aug(i)}). \quad (7)$$

Similar to the self-supervised loss L_{self} , we do not directly adopt the consistency regularization loss L_{reg} to optimize the recognition model, but integrate them using cross-match loss, which would reduce the computation loads.

5) *Cross-match Loss*: While minimizing L_{self} and L_{reg} during training can make effective use of the unlabeled target domain data, optimizing the consistency regularization loss and self-supervised loss separately would greatly increase the computation loads of the proposed framework. To resolve this problem, we have noted that both two losses contain the predictions $\hat{\mathbf{y}}_t$, which looks like a “bridge” connecting the pseudo labels \mathbf{y}_t^p and the predictions $\hat{\mathbf{y}}_t^{aug}$. Inspired by this, we take out the “bridge” $\hat{\mathbf{y}}_t$ from the two losses and directly compute the discrepancies between the pseudo labels \mathbf{y}_t^p and the predictions $\hat{\mathbf{y}}_t^{aug}$, which intuitively is equivalent to merge L_{self} and L_{reg} into one loss namely cross-match loss L_u as Fig. 3 shown. The loss L_u is computed as follows:

$$L_u = -\frac{1}{P} \sum_{i=1}^P \mathbf{y}_t^{p(i)} \cdot \log(\hat{\mathbf{y}}_t^{aug(i)}), \quad (8)$$

where P is the number of pseudo label, $\mathbf{y}_t^{p(i)}$ is the pseudo labels, $\hat{\mathbf{y}}_t$ denotes the predictions of augmented version data.

6) *Confidence Constraint Loss*: The confidence constraint loss L_c is designed to attenuate the negative effects of incorrect pseudo labels on recognition model. In the proposed framework, obtaining the pseudo labels of the unlabeled target

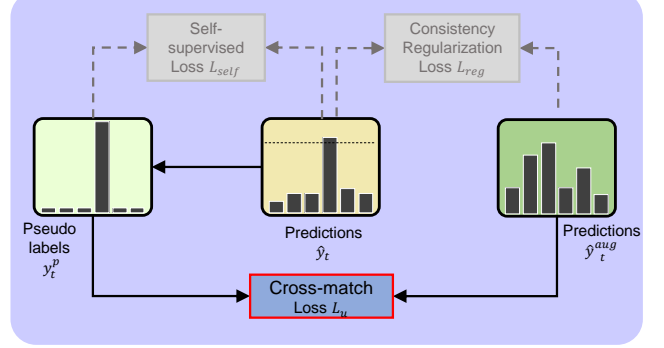


Fig. 3. The cross-match loss L_u is obtained by integrating the self-supervised loss L_{self} and the consistency regularization loss L_{reg} .

domain data and utilizing them to training the model is effective. However, the existing work shows that incorrect pseudo labels is inevitable due to the limitation of the recognition model and the gap between source domain and target domain. According to [81], [82], utilizing the incorrect pseudo labels to train the recognition model would suffer from significant performance degradation. Moreover, the early work [83] shows that enforcing a model to be very confident on only one of the class during training with the pseudo labels can hurt the learning behavior.

Thus, we design a confident constraint loss to encourage the smoothness of output probabilities and prevent overconfident prediction during training. Specifically, as shown in Fig. 4, we compute Kullback-Leibler (KL) divergence between the predictions $\hat{\mathbf{y}}_t$ and the matrix \mathbf{J} to measure the discrepancies between the matrix \mathbf{J} and the predictions $\hat{\mathbf{y}}_t$, where \mathbf{J} is a matrix where every entry is equal to one. Adopting the KL divergence as the confidence constraint loss and minimizing the loss during training would increase the similarity between the matrix \mathbf{J} and the predictions $\hat{\mathbf{y}}_t$, which encourages the smoothness of $\hat{\mathbf{y}}_t$ like the distribution of \mathbf{J} . The loss is computed as follows:

$$L_c = \frac{1}{P} \sum_{i=1}^P \mathbf{J} \cdot \log(\mathbf{J}) - \mathbf{J} \cdot \log(\hat{\mathbf{y}}_t^{(i)}), \quad (9)$$

where P is the number of pseudo labels, $\hat{\mathbf{y}}_t$ denotes the predictions of the model on target domain.

7) *Data Augmentation Methods*: In this paper, data augmentation methods are adopted to obtain the augmented version of the unlabeled target domain data, which is necessary to the consistency regularization. Unlike optical images, the semantic information in RF signals are usually not interpretable intuitively, and the data augmentation methods [33] including flipping and rotating for optical images would change the spatial information in RF signals, which would be harmful to model training. Moreover, we note that the features pre-processed from RF signals contain a lot of random noises and multi-path effects in spatial dimension, and plenty of redundant information in temporal dimension. Therefore, we propose the two data augmentation methods: *Local Feature*

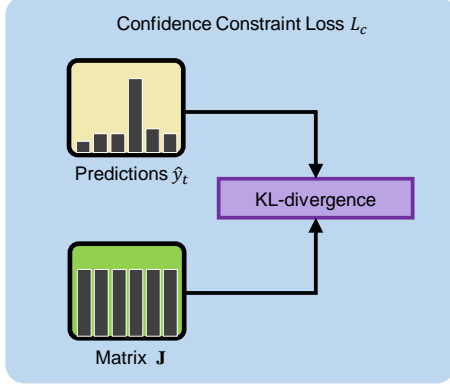


Fig. 4. Confidence Constraint Loss L_c : the Kullback-Leibler (KL) divergence between the predictions \hat{y}_t and the matrix J .

Erasing and Time Erasing to strength the effectiveness of the consistency regularization.

(1) Local Feature Erasing: During training, the neural networks tend to pay more attention to the local features containing too much domain information, which leads to the performance degradation. To address the problem, we force the recognition model to focus on the overall features associated with the gesture category by removing the local features. Specifically, In Fig. 5(a), after the informative features (marked by red box) being detected using CFAR [84] algorithm, part of them are selected to erase by making the value be zero, which are denoted by the erased areas.

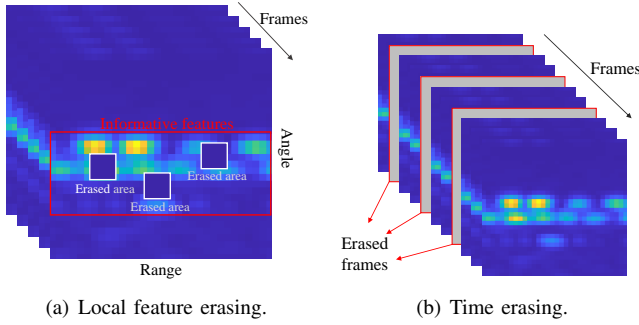


Fig. 5. Our two data augmentation methods.

(2) Time Erasing: Deep neural networks are prone to overfitting without sufficient data, which usually leads to disappointing performance. Increasing the number and diversity of gesture samples is helpful to model training. An effective method is erasing the frames in time dimension, which simulates gesture in different velocities. As Fig. 5(b) shown, the time erasing selects some frames to remove and padding with zero, which are denoted by the gray frames in Fig. 5(b).

C. Objective and Training

The final objective function is composed of supervised loss L_s , cross-match loss L_u , and constraint loss L_c . The objective function is defined as follows:

$$L = L_s + \lambda L_u + \eta L_c, \quad (10)$$

where λ, η are predefined weight of the losses. During training, we compute and minimize the objective function to update the parameters of neural network according to SGD [35].

V. EXPERIMENTS

In this section, we conduct extensive experiments on two different RF-based gesture recognition datasets, i.e., WiFi and mmWave datasets, to evaluate the performance of the proposed framework.

A. Experiment with WiFi Signals

1) *Dataset*: We evaluate the proposed framework on the public Widar 3.0 [17] dataset. The dataset is collected from 3 rooms, 16 users, 5 locations and 5 orientations, which contains 6 gesture categories (i.e., Push & Push, Sweep, Clap, Slide, Draw circle and Draw zigzag) as shown in Fig. 6(c). In total, the dataset includes 11250 data samples (15 users \times 5 locations \times 5 orientations \times 6 gestures \times 5 instances). The layouts and sensing areas of the three different experiment environments (i.e., classroom, hall and office) are shown in Fig. 6(a), and the locations and orientations of subjects are shown in Fig 6(b).

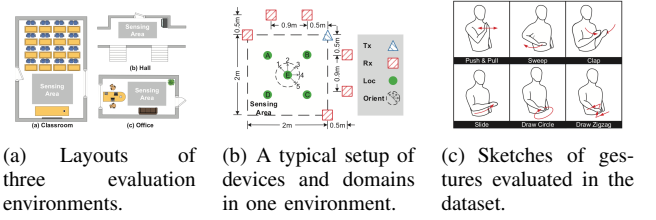


Fig. 6. The setup of WiFi dataset [17].

2) *Data Preprocessing*: In this experiment, the WiFi signals are first processed to the body coordinates profile (BVP) feature as in Widar 3.0 [17]. BVP is the matrix with dimension as $V_x \times V_y \times T$, where V_x and V_y are the number of possible values of velocity components decomposed along each axis of the body coordinates, T is the number of BVP snapshots.

To better understand the BVP and show the differences between the WiFi-based gestures, we randomly select the BVP of the two gestures (Draw circle and Draw zigzag) and visualize them in Fig. 7. Fig. 7 (a) and Fig. 7 (b) show the differences in draw circle and draw zigzag, which indicates there are differences in spatial dimension and temporal dimension between different gestures. Moreover, Fig. 7 (b) Fig. 7 (c) denote the same gesture (draw zigzag) but collected from different locations. We easily find the discrepancies in the gesture from different domains, which are harmful to our recognition model.

3) *Baseline Methods*: We compare our approach with three deep learning models including CrossSense [18], EI [19] and Widar3.0 [17]. Specifically, CrossSense proposes an ANN-based roaming model to translate signal features from source domains to target domains, and employs multiple expert models for gesture recognition. EI is the domain adaptation scheme based on adversarial learning. In Widar 3.0 [17], the authors

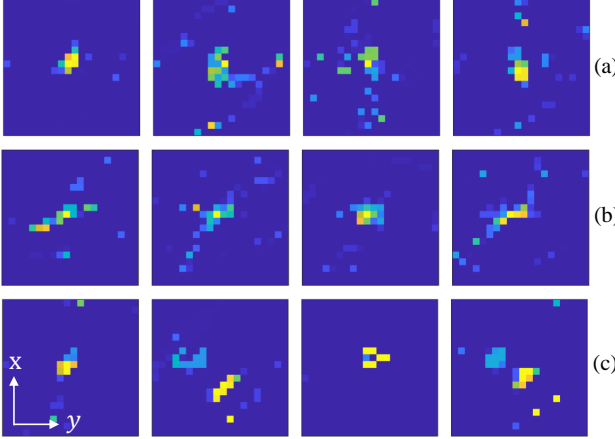


Fig. 7. The BVP of the gesture draw circle and draw zigzag. (a) BVP of the gesture draw circle; (b) BVP of the gesture draw zigzag; (c) BVP of the gesture draw zigzag in other location; Columns represent time series of 4 frames. In BVP, pixel color, x-axis and y-axis correspond to doppler power, horizontal velocity, vertical velocity, respectively.

extract the domain invariant feature BVP based on DFS data and feed them into a model combining CNN and GRUs, which is state-of-the-art method.

4) Cross Domain Evaluation: We evaluate the performance of our framework on cases crossing different domain factors, including orientation, location, subject, and environment. When we evaluate on each domain factor, we keep the others unchanged. For each domain factor, we adopt one domain as the target domain, and the other domains as the source domain. We train the recognition model using source domain data with labels and target domain data without labels, then test the recognition model on the target domain. We conduct experiments using all the baseline methods for comparison.

The overall performance of our framework on WiFi dataset in four domains is shown in Fig. 8. In the figure, the accuracy denotes the average accuracy of every domains and we can see that our framework achieves the highest accuracy in all domains comparing with other baseline methods, which demonstrates the effectiveness of our framework on WiFi dataset. Besides, the detailed performance of our framework in four domains (orientation, location, subject, and environment) are shown below. The numbers or letters behind the arrow \rightarrow represent the target domain.

(1) Cross Orientation: In this experiment, we adopt one orientation domain as the target domain and the other 4 orientations as the source domains. Table I shows that the proposed framework has an average accuracy of 87.21%, which is the highest average accuracy comparing to other methods. We also note that the framework has an improvement of 4.35% over Widar 3.0 and achieves accuracy over 90% on orientation 2 and 3. Even though the proposed framework achieves significant performance improvements on all orientations, the accuracy of orientation 5 is not very high, the reason is that the subjects in orientation 5 are too far away from the center, which are not captured full information of gestures by the WiFi devices.

(2) Cross Location: Similar to the cross orientation settings,

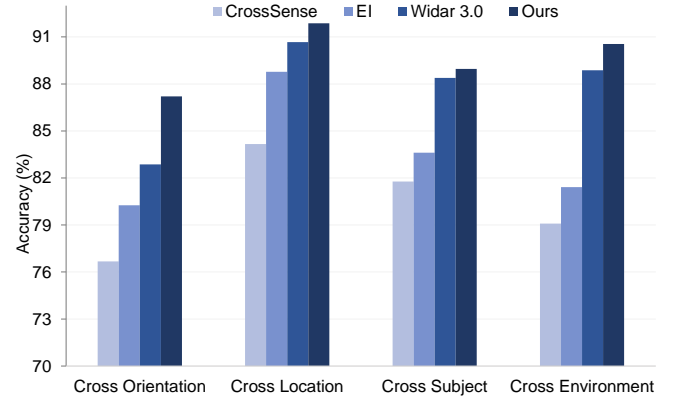


Fig. 8. The overall performance of our framework on WiFi dataset.

TABLE I
CROSS ORIENTATION ACCURACY (%)

| Methods | $\rightarrow 1$ | $\rightarrow 2$ | $\rightarrow 3$ | $\rightarrow 4$ | $\rightarrow 5$ | Avg |
|------------|-----------------|-----------------|-----------------|-----------------|-----------------|--------------|
| CrossSense | 69.41 | 80.23 | 80.45 | 83.18 | 70.07 | 76.67 |
| EI | 70.42 | 81.15 | 88.16 | 90.83 | 70.74 | 80.26 |
| Widar 3.0 | 80.24 | 89.64 | 89.05 | 82.75 | 72.64 | 82.86 |
| Ours | 87.44 | 91.64 | 91.98 | 85.46 | 79.53 | 87.21 |

we adopt data from 4 locations as the source domains, and the data from the last location as the target domain. The results are shown in Table II. Compared with other methods, our framework achieves the highest average accuracy of 91.87%. And location E has the highest accuracy of 95.86%. We also note that the accuracy of all locations is above 90%.

TABLE II
CROSS LOCATION ACCURACY (%)

| Methods | $\rightarrow A$ | $\rightarrow B$ | $\rightarrow C$ | $\rightarrow D$ | $\rightarrow E$ | Avg |
|------------|-----------------|-----------------|-----------------|-----------------|-----------------|--------------|
| CrossSense | 88.61 | 85.23 | 82.89 | 78.94 | 85.16 | 84.16 |
| EI | 87.91 | 90.13 | 86.85 | 85.82 | 93.14 | 88.77 |
| Widar 3.0 | 89.14 | 89.10 | 90.50 | 89.50 | 95.15 | 90.67 |
| Ours | 90.47 | 90.30 | 92.30 | 90.44 | 95.86 | 91.87 |

(3) Cross Subject: Data collected from different subjects may have discrepancies due to their various behavior patterns and body shapes, which weakens the performance of recognition model on different subjects. To evaluate the performance of the framework in subject domain, we conduct the experiments. To be specific, we adopt the data from 1 user as the target domain and 6 users' data as the source domains. The results in Table III show our framework achieves the highest average accuracy of 88.96%.

(4) Cross Environment: To evaluate the performance of our framework in environment domain, we use the gesture data collected in 2 rooms as the source domains data and the other one as the target domain. The results in Table IV show that the framework has an overall accuracy of 90.55%, which is the highest average accuracy.

TABLE III
CROSS SUBJECT ACCURACY (%)

| Methods | →U10 | → U11 | → U12 | → U13 | → U14 | → U15 | → U16 | → U17 | Avg |
|------------|--------------|--------------|--------------|--------------|--------------|--------------|--------------|--------------|--------------|
| CrossSense | 77.67 | 81.35 | 80.24 | 83.73 | 85.97 | 82.43 | 80.19 | 82.59 | 81.77 |
| EI | 80.11 | 83.56 | 85.91 | 82.05 | 84.36 | 85.44 | 81.23 | 86.21 | 83.61 |
| Widar 3.0 | 86.26 | 90.13 | 83.33 | 89.86 | 87.73 | 89.97 | 91.46 | 88.34 | 88.38 |
| Ours | 86.79 | 89.73 | 80.93 | 91.60 | 88.13 | 92.51 | 91.33 | 90.67 | 88.96 |

TABLE IV
CROSS ENVIRONMENT ACCURACY (%)

| Methods | → Room 1 | → Room 2 | → Room 3 | Avg |
|------------|--------------|--------------|--------------|--------------|
| CrossSense | 72.78 | 81.75 | 82.76 | 79.09 |
| EI | 75.73 | 84.54 | 83.98 | 81.42 |
| Widar 3.0 | 81.58 | 93.47 | 91.08 | 88.87 |
| Ours | 83.93 | 94.88 | 92.85 | 90.55 |

In summary, our framework achieves state-of-the-art performance on WiFi dataset in four domains (locations, orientations, subjects and environments), which demonstrates the effectiveness of our framework on WiFi dataset. Furthermore, our framework not only achieves the considerable results on WiFi dataset, but also performs very well on mmWave dataset, which is presented below.

B. Experiment with mmWave Signals

1) *Dataset*: We adopt a public mmWave dataset [80], which is collected from 25 volunteers, 6 environments and 5 locations to evaluate our framework. Fig. 9 illustrates the setup of 5 locations in each environment. The dataset contains 6 common gestures including Push, Pull, Left swipe, Right swipe, Clockwise turning and Anticlockwise turning. Each volunteer is asked to perform each kind of gesture 5 times at each location. In total, the dataset includes 10800 data samples.

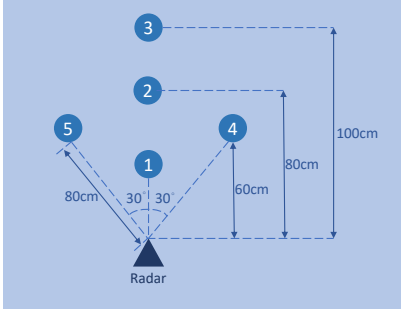


Fig. 9. The setup of 5 locations in each environment [80].

2) *Data Preprocessing*: In this experiment, the mmWave signals are processed to the Dynamic Range Angle Image sequence (DRAI) as in [80], which is the matrix with dimension $N \times M \times T$. Specifically, as shown in Fig. 10, the 3D-FFT is adopted on raw signals to derive the ranges, velocities and angles of hands. Then, the noise elimination is used to filter environmental interference and improve the robustness of the

recognition model. After that, we adopt the DRAI as the input of the recognition model.



Fig. 10. The calculation process of DRAI sequences.

To better describe the DRAI and show the differences in different gestures and different domains, we randomly visualize the DRAI of the two gestures (e.g., Slide right and Slide left) in Fig. 11. Fig. 11 (a) and Fig. 11 (b) denote the two gesture collected from same settings, from which, we can see that the feature information of a gesture consists of temporal and spatial information. Furthermore, Fig. 11 (b) Fig. 11 (c) represent the same gesture (slide left) collected from different locations, in which, the discrepancies are observed.

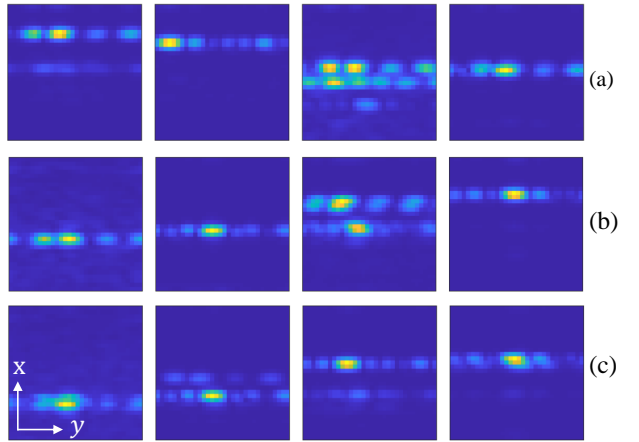


Fig. 11. DRAI of the gesture slide right and slide left. (a) DRAI of the gesture slide right; (b) DRAI of the gesture slide left; (c) DRAI of the gesture slide left in other location; Columns represent time series of 4 frames. In DRAI, pixel color, x-axis and y-axis correspond to doppler power, AoA, range, respectively.

3) *Baseline Methods*: We compare our approach with two deep learning models RadarNet [46] and Widar3.0 [17]. Specifically, RadarNet designs an efficient neural network and trains a robust model. We first process the mmWave radar signals to Range Doppler Image, then use the Range Doppler Image as the RadarNet model's input. In Widar 3.0 paper, the authors feed the features into a gesture recognition model combining CNNs and GRUs. In this paper, we adopt the gesture recognition model as the another baseline and utilize the DRAI as the input.

4) *Cross Domain Evaluation*: We evaluate the performance of the proposed framework on mmWave dataset in different domains including location, subject, and environment. When evaluating on each domain factor, we keep the other domain factors unchanged. For each domain factor, we adopt one domain as the target domain and the others as the source domain. We utilize the source domain data with labels and the target domain data without labels to train the recognition model, and test the recognition model on the target domain. We

conduct experiments using all the baseline methods to validate the effectiveness of our framework.

The overall performance of our framework on mmWave dataset in three domains is shown in Fig. 12. In the figure, the accuracy denotes the average accuracy of every domains, and our framework achieves the highest accuracy in all domains comparing with other baseline methods, which demonstrates the effectiveness of our framework on mmWave dataset. Besides, the detailed performance of our framework in different domains are shown below. The numbers or letters behind the arrow \rightarrow represent the target domain.

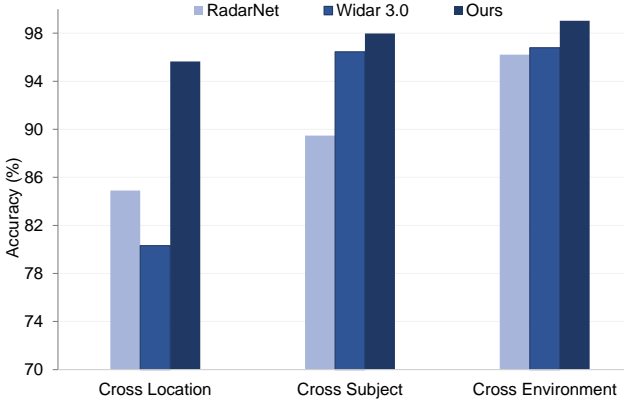


Fig. 12. The overall performance of our framework on mmWave dataset.

(1) *Cross Location*: To evaluate our framework's performance of crossing location, we use data of 4 locations as the source domains, and the data of last location as the target domain. In Table V, L1 - L5 represent the five locations of subject. The results are shown in Table V. Compared with other methods, our framework achieves the highest average accuracy of 95.65% and has significant improvement of 15.23% over the Widar 3.0 and 10.75% over RadarNet. Location 2 has the highest accuracy of 98.84%.

TABLE V
CROSS LOCATION ACCURACY (%)

| Methods | \rightarrow L1 | \rightarrow L2 | \rightarrow L3 | \rightarrow L4 | \rightarrow L5 | Avg |
|-----------|------------------|------------------|------------------|------------------|------------------|--------------|
| RadarNet | 67.69 | 96.81 | 69.77 | 95.19 | 95.05 | 84.90 |
| Widar 3.0 | 80.13 | 97.45 | 82.59 | 75.92 | 65.65 | 80.32 |
| Ours | 91.20 | 98.84 | 94.30 | 96.94 | 96.95 | 95.65 |

(2) *Cross Subject*: Different subjects' data may show discrepancies due to their unique behavior patterns and body shapes. To evaluate on the subjects, we use data from User 1-6 to evaluate the framework. Each time, we adopt the data from 1 user as the target domain and the other users' data as the source domains. The results in Table VI show that our framework achieves the highest average accuracy of 97.97%. We also note that all subjects have the accuracy above 93%, and User 1-2 have the accuracy above 99%, which demonstrates the impressive performance of our framework.

(3) *Cross Environment*: Different rooms have different layouts, which has an influence on signals propagation. To

TABLE VI
CROSS SUBJECT ACCURACY (%)

| Methods | \rightarrow U1 | \rightarrow U2 | \rightarrow U3 | \rightarrow U4 | \rightarrow U5 | \rightarrow U6 | Avg |
|-----------|------------------|------------------|------------------|------------------|------------------|------------------|--------------|
| RadarNet | 95.06 | 92.93 | 83.06 | 85.20 | 90.26 | 90.40 | 89.48 |
| Widar 3.0 | 98.80 | 98.13 | 91.85 | 98.33 | 98.83 | 92.78 | 96.45 |
| Ours | 99.42 | 99.02 | 93.28 | 99.33 | 98.83 | 96.90 | 97.97 |

evaluate on the different environments, we use the gesture samples collected in five rooms as the source domains data and the last one as the target domain. E1 - E6 represent the six environments. The results in Table VII show that the framework achieves an overall accuracy of 99.04%, which is the highest among different methods. Moreover, our framework achieves an improvement of 2.25% over the Widar 3.0 and 2.83% over the RadarNet.

TABLE VII
CROSS ENVIRONMENT ACCURACY (%)

| Methods | \rightarrow E1 | \rightarrow E2 | \rightarrow E3 | \rightarrow E4 | \rightarrow E5 | \rightarrow E6 | Avg |
|-----------|------------------|------------------|------------------|------------------|------------------|------------------|--------------|
| RadarNet | 99.09 | 97.11 | 92.47 | 98.66 | 98.00 | 91.93 | 96.21 |
| Widar 3.0 | 97.33 | 98.53 | 94.80 | 95.06 | 98.13 | 96.93 | 96.79 |
| Ours | 99.19 | 98.93 | 98.66 | 99.46 | 98.93 | 99.06 | 99.04 |

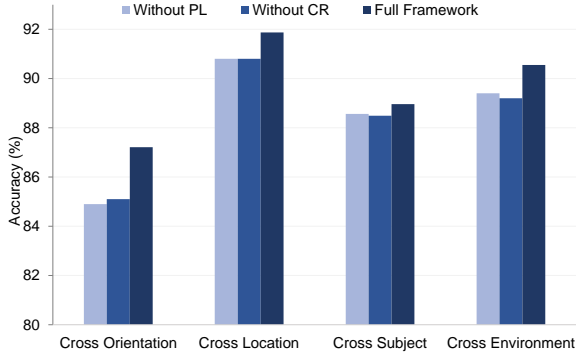
In conclusion, similar to the experiments on WiFi dataset, our framework achieves considerable performance on mmWave radar dataset, which shows that our framework is an effective and general framework that can be used to improve the accuracy of the gesture recognition model with different RF signals.

C. Ablation Experiments

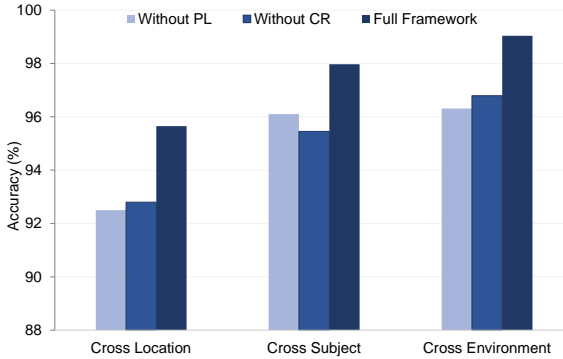
In this section, we perform extensive ablation studies to evaluate the impact of all modules of the proposed framework.

1) *Impact of Pseudo-labeling and Consistency Regularization*: The performance gain of our framework mainly comes from two modules: pseudo-labeling and consistency regularization. To evaluate which component is essential, we perform two ablation experiments on WiFi dataset and mmWave dataset. Specifically, we remove the consistency regularization module and the pseudo-labeling module from full framework, respectively and keep the other settings unchanged. In Fig. 13, “Without CR” represents the framework whose consistency regularization module is removed, “Without PL” represents the framework whose pseudo-labeling module is removed, and the accuracy is the average accuracy of each domain. From Fig. 13, we can see that the performance of both two incomplete framework is limited, which indicates that both techniques are critical to the proposed framework.

2) *Impact of Cross-match Loss*: To better understand the efficiency of the cross-match loss L_u , we conduct the experiments on WiFi dataset and mmWave dataset on NVIDIA A100-PCIE-40GB GPU. Specifically, we first deploy our framework with the self-supervised loss L_{self} and the consistency regularization loss L_{reg} . Then, we deploy our framework only with the cross-match loss L_u . We keep the other



(a) The Impact of Pseudo-labeling and Consistency Regularization on WiFi Dataset



(b) The Impact of Pseudo-labeling and Consistency Regularization on mmWave Dataset

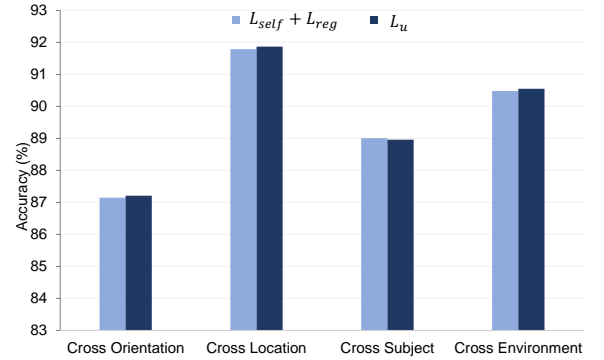
Fig. 13. The Impact of Pseudo-labeling and Consistency Regularization.

settings unchanged and evaluate the performance in terms of classification accuracy and training time. From Fig. 14, we can see that the classification accuracy of the two methods are so close. Moreover, in Table VIII, the framework only with cross-match loss L_u needs shorter training time than the framework adopting the two losses L_{self} and L_{reg} . In conclusion, the cross-match loss L_u makes the whole framework efficient while maintaining the effectiveness.

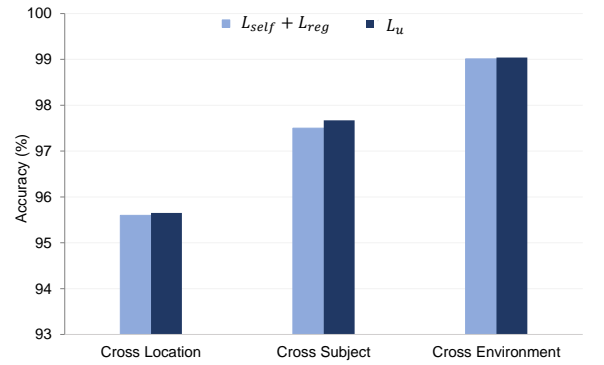
TABLE VIII
THE TRAINING TIME OF THE TWO LOSSES AND THE CROSS-MATCH LOSS.

| Loss | Training Time (second / epoch) |
|----------------------|--------------------------------|
| $L_{self} + L_{reg}$ | 32.5 |
| L_u | 27.4 |

3) *Impact of Confidence Constraint Loss*: In this subsection, we conduct the ablation experiments on WiFi dataset and mmWave dataset to understand whether our framework can achieve the effective performance without confidence constraint L_c . To be specific, we compare the full framework with the framework without confidence constraint L_c . Fig. 15 shows that the performance of the framework without the confidence constraint drops rapidly, which indicates that the confidence constraint is necessary and effective to our framework.

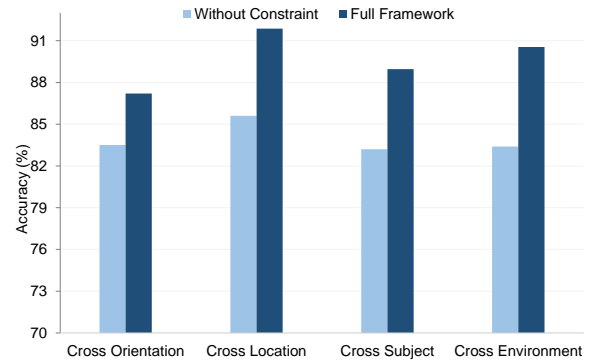


(a) The performance of cross-match loss L_u on WiFi dataset.

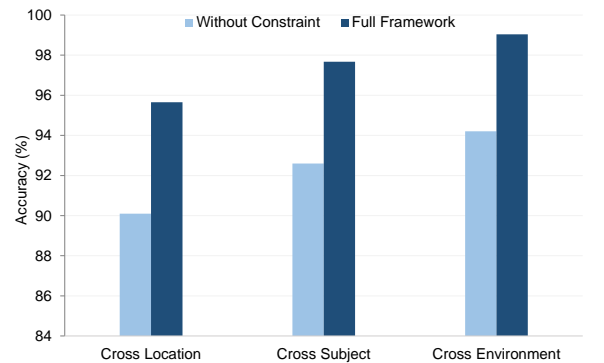


(b) The performance of cross-match loss L_u on mmWave dataset.

Fig. 14. The performance of cross-match loss L_u .



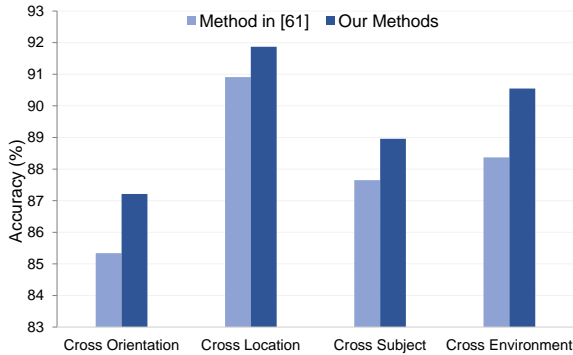
(a) Impact of confidence constraint on WiFi dataset



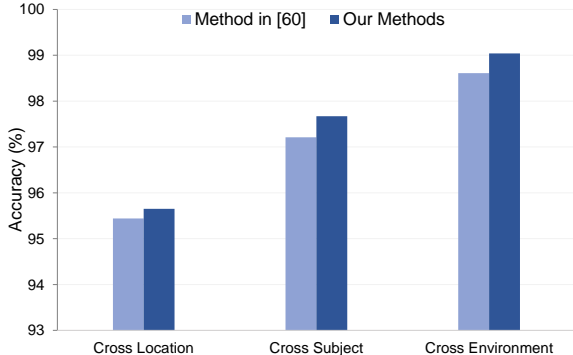
(b) Impact of confidence constraint on mmWave dataset

Fig. 15. Impact of confidence constraint L_c .

4) *Impact of Data Augmentation*: In this work, data augmentation methods are utilized to generate different versions of unlabeled target domain data, which is important to consistency regularization. To demonstrate the effectiveness of the proposed data augmentation method, we compare with WiFi-based method [34] and mmWave-based method [80] on WiFi dataset [17] and mmWave dataset [80], and keep other modules of our framework unchanged. As shown in Fig. 16, the proposed framework with the proposed methods achieves higher accuracy. At the same time, we clearly point out that our augmentation methods are designed for our UDA framework, so that our augmentation methods maybe not applicable to other tasks and other features.



(a) The accuracy of the WiFi-based methods and our methods.

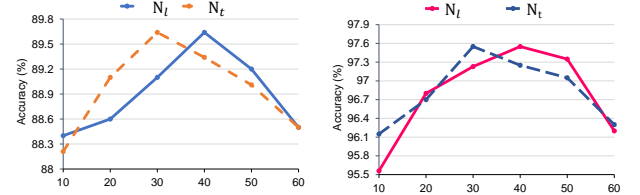


(b) The accuracy of DI-Gesture-Lite and our methods.

Fig. 16. The comparison with other data augmentation methods.

Furthermore, for local feature erasing, we select $N_l\%$ informative features randomly and erase them by making their value equal to zero. For time erasing, we remove $N_t\%$ time frames of the feature matrix randomly. In this work, the N_l is experimentally set as 40 and the N_t is experimentally set as 30. To investigate the impact of the number of deleted features, we tune N_l and N_t from 10 to 60 and keep other settings unchanged. The Fig. 17 shows that the highest accuracy is obtained when the N_l is 40 and the N_t is 30. In a nutshell, the deleted features are not the more the better. An appropriate number of the deleted features would enhance the performance of our data augmentation methods.

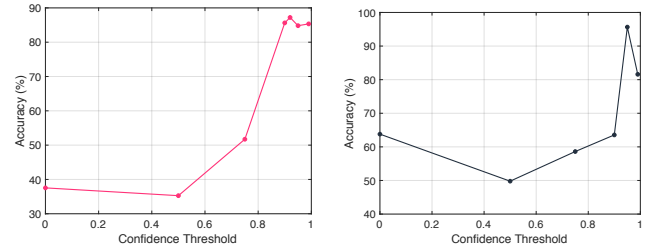
5) *Impact of Pseudo Label Threshold*: In our framework, we adopt pseudo-labeling method to obtain the pseudo labels of the unlabeled target domain data. To be specific, we utilize the threshold τ to select the highly confident predictions as



(a) The accuracy of different N_l and N_t on WiFi dataset. (b) The accuracy of different N_l and N_t on mmWave dataset.

Fig. 17. Impact of the number of deleted features.

the pseudo labels. In this sub-section, we study the impact of different threshold values. We conduct the analysis experiments on WiFi dataset and mmWave dataset. We set the threshold values ranging from 0 to 0.99 and remain the other settings unchanged. In Fig. 18, the accuracy corresponding to each threshold is the average result of each dataset. The Fig. 18(a) shows The performance of the framework on WiFi dataset improves with the threshold increasing and achieves the highest accuracy when the threshold value is 0.92. The Fig. 18(b) shows that the highest accuracy on mmWave dataset is obtained when the threshold value is 0.95. In a word, a appropriate threshold is helpful to our framework, which could be obtained experimentally.



(a) The accuracy of different threshold τ on WiFi dataset. (b) The accuracy of different threshold τ on mmWave dataset.

Fig. 18. Impact of Confidence Threshold.

D. The efficiency of the proposed framework

In this section, we investigate the efficiency of the proposed framework. To be specific, we compare the Floating Point Operations (FLOPs), training time and testing time of our framework with the backbone model, which is summarized in Table IX. Compared with the backbone, the proposed framework only increase 18.5% FLOPs. Moreover, we also evaluate the training time per epoch and testing time on NVIDIA A100-PCIE-40GB GPU as shown in Table IX. From Table. IX, we can see that the training time of our framework is slightly longer than that of the backbone, while the testing time keeps the same. We note that there are two reasons about this. One reason is that our method adds the unlabeled target domain data to the training dataset, which leads to more time to train the neural network. The other reason is that the data augmentation operation adds training time.

TABLE IX
THE FLOPs, TRAINING TIME AND TESTING TIME OF THE BACKBONE AND
OUR FRAMEWORK.

| Method | FLOPs (M) | Training time (s / epoch) | Testing time (s) |
|---------------|-------------|---------------------------|------------------|
| Backbone | 1.03 | 23.1 | 1.01 |
| Our framework | 1.22 | 27.4 | 1.01 |

VI. CONCLUSION

In this paper, we proposed an unsupervised domain adaptation framework for RF-based gesture recognition to enhance the performance of the recognition model on the unlabeled target domain. We proposed a pseudo-labeling method and consistency regularization to utilize unlabeled data for model training and align the output distribution for enhancing the robustness of neural network. Then we proposed a cross-match loss to integrate the pseudo-labeling and consistency regularization, which makes the whole framework simple yet effective. Moreover, we design a confidence constraint loss and two data augmentation methods to improve the performance of our framework. Finally, we conducted experiments on two different RF gesture recognition testbeds, i.e., WiFi and mmWave signals, to evaluate the performance of the proposed framework. The experimental results demonstrated the superiority of our framework over existing ones. We believe that the proposed framework can not only improve the performance of gesture recognition, but also facilitate more investigations towards unsupervised learning with wireless signals.

REFERENCES

- [1] M. Wang, B. Ni, and X. Yang, “Recurrent modeling of interaction context for collective activity recognition,” in *Proceedings of the IEEE Conference on Computer Vision and Pattern Recognition*, 2017, pp. 3048–3056.
- [2] G. Gkioxari, R. Girshick, P. Dollár, and K. He, “Detecting and recognizing human-object interactions,” in *Proceedings of the IEEE Conference on Computer Vision and Pattern Recognition*, 2018, pp. 8359–8367.
- [3] T. Li, Q. Liu, and X. Zhou, “Practical human sensing in the light,” in *Proceedings of the 14th Annual International Conference on Mobile Systems, Applications, and Services*, 2016, pp. 71–84.
- [4] A. Bulling, U. Blanke, and B. Schiele, “A tutorial on human activity recognition using body-worn inertial sensors,” *ACM Computing Surveys (CSUR)*, vol. 46, no. 3, pp. 1–33, 2014.
- [5] Y. Guan and T. Plötz, “Ensembles of deep lstm learners for activity recognition using wearables,” *Proceedings of the ACM on Interactive, Mobile, Wearable and Ubiquitous Technologies*, vol. 1, no. 2, pp. 1–28, 2017.
- [6] S. Shen, H. Wang, and R. Roy Choudhury, “I am a smartwatch and i can track my user’s arm,” in *Proceedings of the 14th annual international conference on Mobile systems, applications, and services*, 2016, pp. 85–96.
- [7] R. Nandakumar, A. Takakuwa, T. Kohno, and S. Gollakota, “Coverband: Activity information leakage using music,” *Proceedings of the ACM on Interactive, Mobile, Wearable and Ubiquitous Technologies*, vol. 1, no. 3, pp. 1–24, 2017.
- [8] K. Yatani and K. N. Truong, “Bodyscope: a wearable acoustic sensor for activity recognition,” in *Proceedings of the 2012 ACM Conference on Ubiquitous Computing*, 2012, pp. 341–350.
- [9] J. Wang, Q. Gao, M. Pan, and Y. Fang, “Device-free wireless sensing: Challenges, opportunities, and applications,” *IEEE Network*, vol. 32, no. 2, pp. 132–137, 2018.
- [10] S. Savazzi, S. Sigg, M. Nicoli, V. Rampa, S. Kianoush, and U. Spagnolini, “Device-free radio vision for assisted living: Leveraging wireless channel quality information for human sensing,” *IEEE Signal Processing Magazine*, vol. 33, no. 2, pp. 45–58, 2016.
- [11] Z. Zhou, C. Wu, Z. Yang, and Y. Liu, “Sensorless sensing with wifi,” *Tsinghua Science and Technology*, vol. 20, no. 1, pp. 1–6, 2015.
- [12] Y. Wang, J. Liu, Y. Chen, M. Gruteser, J. Yang, and H. Liu, “E-eyes: device-free location-oriented activity identification using fine-grained wifi signatures,” in *Proceedings of the 20th annual international conference on Mobile computing and networking*, 2014, pp. 617–628.
- [13] S. Shi, S. Sigg, W. Zhao, and Y. Ji, “Monitoring attention using ambient fm radio signals,” *IEEE Pervasive Computing*, vol. 13, no. 1, pp. 30–36, 2014.
- [14] W. Wang, A. X. Liu, M. Shahzad, K. Ling, and S. Lu, “Device-free human activity recognition using commercial wifi devices,” *IEEE Journal on Selected Areas in Communications*, vol. 35, no. 5, pp. 1118–1131, 2017.
- [15] Y. Ma, G. Zhou, S. Wang, H. Zhao, and W. Jung, “Signfi: Sign language recognition using wifi,” *Proceedings of the ACM on Interactive, Mobile, Wearable and Ubiquitous Technologies*, vol. 2, no. 1, pp. 1–21, 2018.
- [16] A. Virmani and M. Shahzad, “Position and orientation agnostic gesture recognition using wifi,” in *Proceedings of the 15th Annual International Conference on Mobile Systems, Applications, and Services*, 2017, pp. 252–264.
- [17] Y. Zheng, Y. Zhang, K. Qian, G. Zhang, Y. Liu, C. Wu, and Z. Yang, “Zero-effort cross-domain gesture recognition with wi-fi,” in *Proceedings of the 17th Annual International Conference on Mobile Systems, Applications, and Services*, 2019, pp. 313–325.
- [18] J. Zhang, Z. Tang, M. Li, D. Fang, P. Nurmi, and Z. Wang, “Crosssense: Towards cross-site and large-scale wifi sensing,” in *Proceedings of the 24th Annual International Conference on Mobile Computing and Networking*, 2018, pp. 305–320.
- [19] W. Jiang, C. Miao, F. Ma, S. Yao, Y. Wang, Y. Yuan, H. Xue, C. Song, X. Ma, D. Koutsoukos *et al.*, “Towards environment independent device free human activity recognition,” in *Proceedings of the 24th Annual International Conference on Mobile Computing and Networking*, 2018, pp. 289–304.
- [20] C. Xiao, D. Han, Y. Ma, and Z. Qin, “Csigan: Robust channel state information-based activity recognition with gans,” *IEEE Internet of Things Journal*, vol. 6, no. 6, pp. 10 191–10 204, 2019.
- [21] F. Wang, J. Liu, and W. Gong, “Wicar: Wifi-based in-car activity recognition with multi-adversarial domain adaptation,” in *Proceedings of the International Symposium on Quality of Service*, 2019, pp. 1–10.
- [22] Z. Wang, S. Chen, W. Yang, and Y. Xu, “Environment-independent wi-fi human activity recognition with adversarial network,” in *ICASSP 2021-2021 IEEE International Conference on Acoustics, Speech and Signal Processing (ICASSP)*. IEEE, 2021, pp. 3330–3334.
- [23] H. Kang, Q. Zhang, and Q. Huang, “Context-aware wireless based cross domain gesture recognition,” *IEEE Internet of Things Journal*, 2021.
- [24] X. Ma, Y. Zhao, L. Zhang, Q. Gao, M. Pan, and J. Wang, “Practical device-free gesture recognition using wifi signals based on metalearning,” *IEEE Transactions on Industrial Informatics*, vol. 16, no. 1, pp. 228–237, 2019.
- [25] M. Sajjadi, M. Javanmardi, and T. Tasdizen, “Regularization with stochastic transformations and perturbations for deep semi-supervised learning,” *Advances in neural information processing systems*, vol. 29, pp. 1163–1171, 2016.
- [26] A. Tarvainen and H. Valpola, “Mean teachers are better role models: Weight-averaged consistency targets improve semi-supervised deep learning results,” *arXiv preprint arXiv:1703.01780*, 2017.
- [27] K. Sohn, D. Berthelot, C.-L. Li, Z. Zhang, N. Carlini, E. D. Cubuk, A. Kurakin, H. Zhang, and C. Raffel, “Fixmatch: Simplifying semi-supervised learning with consistency and confidence,” *arXiv preprint arXiv:2001.07685*, 2020.
- [28] Q. Xie, Z. Dai, E. Hovy, M.-T. Luong, and Q. V. Le, “Unsupervised data augmentation for consistency training,” *arXiv preprint arXiv:1904.12848*, 2019.
- [29] D.-H. Lee *et al.*, “Pseudo-label: The simple and efficient semi-supervised learning method for deep neural networks,” in *Workshop on challenges in representation learning, ICML*, vol. 3, no. 2, 2013, p. 896.
- [30] R. Gopalan, R. Li, and R. Chellappa, “Domain adaptation for object recognition: An unsupervised approach,” in *2011 international conference on computer vision*. IEEE, 2011, pp. 999–1006.
- [31] J. Na, H. Jung, H. J. Chang, and W. Hwang, “Fixbi: Bridging domain spaces for unsupervised domain adaptation,” in *Proceedings of the IEEE/CVF Conference on Computer Vision and Pattern Recognition*, 2021, pp. 1094–1103.
- [32] M. Long, H. Zhu, J. Wang, and M. I. Jordan, “Unsupervised domain adaptation with residual transfer networks,” *arXiv preprint arXiv:1602.04433*, 2016.

[33] C. Shorten and T. M. Khoshgoftaar, "A survey on image data augmentation for deep learning," *Journal of Big Data*, vol. 6, no. 1, pp. 1–48, 2019.

[34] J. Zhang, F. Wu, B. Wei, Q. Zhang, H. Huang, S. W. Shah, and J. Cheng, "Data augmentation and dense-lstm for human activity recognition using wifi signal," *IEEE Internet of Things Journal*, vol. 8, no. 6, pp. 4628–4641, 2020.

[35] N. Qian, "On the momentum term in gradient descent learning algorithms," *Neural networks*, vol. 12, no. 1, pp. 145–151, 1999.

[36] J. Wang, H. Jiang, J. Xiong, K. Jamieson, X. Chen, D. Fang, and B. Xie, "Lifs: Low human-effort, device-free localization with fine-grained subcarrier information," in *Proceedings of the 22nd Annual International Conference on Mobile Computing and Networking*, 2016, pp. 243–256.

[37] X. Li, D. Zhang, Q. Lv, J. Xiong, S. Li, Y. Zhang, and H. Mei, "Indotrack: Device-free indoor human tracking with commodity wifi," *Proceedings of the ACM on Interactive, Mobile, Wearable and Ubiquitous Technologies*, vol. 1, no. 3, pp. 1–22, 2017.

[38] K. Kalgaonkar and B. Raj, "One-handed gesture recognition using ultrasonic doppler sonar," in *2009 IEEE International Conference on Acoustics, Speech and Signal Processing*. IEEE, 2009, pp. 1889–1892.

[39] X. Huang and M. Dai, "Indoor device-free activity recognition based on radio signal," *IEEE Transactions on Vehicular Technology*, vol. 66, no. 6, pp. 5316–5329, 2016.

[40] J. Lien, N. Gillian, M. E. Karagozler, P. Amihood, C. Schwesig, E. Olson, H. Raja, and I. Poupyrev, "Soli: Ubiquitous gesture sensing with millimeter wave radar," *ACM Transactions on Graphics (TOG)*, vol. 35, no. 4, pp. 1–19, 2016.

[41] S. Zhu, J. Xu, H. Guo, Q. Liu, S. Wu, and H. Wang, "Indoor human activity recognition based on ambient radar with signal processing and machine learning," in *2018 IEEE international conference on communications (ICC)*. IEEE, 2018, pp. 1–6.

[42] T. Fan, C. Ma, Z. Gu, Q. Lv, J. Chen, D. Ye, J. Huangfu, Y. Sun, C. Li, and L. Ran, "Wireless hand gesture recognition based on continuous-wave doppler radar sensors," *IEEE Transactions on Microwave Theory and Techniques*, vol. 64, no. 11, pp. 4012–4020, 2016.

[43] X. J. Zhu, "Semi-supervised learning literature survey," 2005.

[44] H. Liu, Y. Wang, A. Zhou, H. He, W. Wang, K. Wang, P. Pan, Y. Lu, L. Liu, and H. Ma, "Real-time arm gesture recognition in smart home scenarios via millimeter wave sensing," *Proceedings of the ACM on Interactive, Mobile, Wearable and Ubiquitous Technologies*, vol. 4, no. 4, pp. 1–28, 2020.

[45] P. S. Santhalingam, A. A. Hosain, D. Zhang, P. Pathak, H. Rangwala, and R. Kushalnagar, "mmasl: Environment-independent asl gesture recognition using 60 ghz millimeter-wave signals," *Proceedings of the ACM on Interactive, Mobile, Wearable and Ubiquitous Technologies*, vol. 4, no. 1, pp. 1–30, 2020.

[46] E. Hayashi, J. Lien, N. Gillian, L. Giusti, D. Weber, J. Yamanaka, L. Bedal, and I. Poupyrev, "Radarnet: Efficient gesture recognition technique utilizing a miniature radar sensor," in *Proceedings of the 2021 CHI Conference on Human Factors in Computing Systems*, 2021, pp. 1–14.

[47] D. Berthelot, N. Carlini, E. D. Cubuk, A. Kurakin, K. Sohn, H. Zhang, and C. Raffel, "Remixmatch: Semi-supervised learning with distribution alignment and augmentation anchoring," *arXiv preprint arXiv:1911.09785*, 2019.

[48] D. Berthelot, N. Carlini, I. Goodfellow, N. Papernot, A. Oliver, and C. Raffel, "Mixmatch: A holistic approach to semi-supervised learning," *arXiv preprint arXiv:1905.02249*, 2019.

[49] X. Zhai, A. Oliver, A. Kolesnikov, and L. Beyer, "S4l: Self-supervised semi-supervised learning," in *Proceedings of the IEEE/CVF International Conference on Computer Vision*, 2019, pp. 1476–1485.

[50] S. Ao, X. Li, and C. Ling, "Fast generalized distillation for semi-supervised domain adaptation," in *Proceedings of the AAAI Conference on Artificial Intelligence*, vol. 31, no. 1, 2017.

[51] K. Saito, D. Kim, S. Sclaroff, T. Darrell, and K. Saenko, "Semi-supervised domain adaptation via minimax entropy," in *Proceedings of the IEEE/CVF International Conference on Computer Vision*, 2019, pp. 8050–8058.

[52] C. Qin, L. Wang, Q. Ma, Y. Yin, H. Wang, and Y. Fu, "Contradictory structure learning for semi-supervised domain adaptation," in *Proceedings of the 2021 SIAM International Conference on Data Mining (SDM)*. SIAM, 2021, pp. 576–584.

[53] D. Li and T. Hospedales, "Online meta-learning for multi-source and semi-supervised domain adaptation," in *European Conference on Computer Vision*. Springer, 2020, pp. 382–403.

[54] L. Yang, Y. Wang, M. Gao, A. Shrivastava, K. Q. Weinberger, W.-L. Chao, and S.-N. Lim, "Mico: Mixup co-training for semi-supervised domain adaptation," *arXiv e-prints*, pp. arXiv–2007, 2020.

[55] S. Ben-David, J. Blitzer, K. Crammer, F. Pereira *et al.*, "Analysis of representations for domain adaptation," *Advances in neural information processing systems*, vol. 19, p. 137, 2007.

[56] I.-H. Jhuo, D. Liu, D. Lee, and S.-F. Chang, "Robust visual domain adaptation with low-rank reconstruction," in *2012 IEEE conference on computer vision and pattern recognition*. IEEE, 2012, pp. 2168–2175.

[57] M. Long, Y. Cao, J. Wang, and M. Jordan, "Learning transferable features with deep adaptation networks," in *International conference on machine learning*. PMLR, 2015, pp. 97–105.

[58] M. Long, H. Zhu, J. Wang, and M. I. Jordan, "Deep transfer learning with joint adaptation networks," in *International conference on machine learning*. PMLR, 2017, pp. 2208–2217.

[59] G. Kang, L. Jiang, Y. Yang, and A. G. Hauptmann, "Contrastive adaptation network for unsupervised domain adaptation," in *Proceedings of the IEEE/CVF Conference on Computer Vision and Pattern Recognition*, 2019, pp. 4893–4902.

[60] E. Tzeng, J. Hoffman, K. Saenko, and T. Darrell, "Adversarial discriminative domain adaptation," in *Proceedings of the IEEE conference on computer vision and pattern recognition*, 2017, pp. 7167–7176.

[61] S. Sankaranarayanan, Y. Balaji, C. D. Castillo, and R. Chellappa, "Generate to adapt: Aligning domains using generative adversarial networks," in *Proceedings of the IEEE Conference on Computer Vision and Pattern Recognition*, 2018, pp. 8503–8512.

[62] J.-Y. Zhu, T. Park, P. Isola, and A. A. Efros, "Unpaired image-to-image translation using cycle-consistent adversarial networks," in *Proceedings of the IEEE international conference on computer vision*, 2017, pp. 2223–2232.

[63] Y. Ganin, E. Ustinova, H. Ajakan, P. Germain, H. Larochelle, F. Laviolette, M. Marchand, and V. Lempitsky, "Domain-adversarial training of neural networks," *The journal of machine learning research*, vol. 17, no. 1, pp. 2096–2030, 2016.

[64] M.-Y. Liu, T. Breuel, and J. Kautz, "Unsupervised image-to-image translation networks," in *Advances in neural information processing systems*, 2017, pp. 700–708.

[65] D. Zhang, Y. Hu, and Y. Chen, "Mtrack: Tracking multiperson moving trajectories and vital signs with radio signals," *IEEE Internet of Things Journal*, vol. 8, no. 5, pp. 3904–3914, 2020.

[66] Y. Chen, H. Deng, D. Zhang, and Y. Hu, "Speednet: Indoor speed estimation with radio signals," *IEEE Internet of Things Journal*, vol. 8, no. 4, pp. 2762–2774, 2020.

[67] Y. He, Y. Chen, Y. Hu, and B. Zeng, "Wifi vision: sensing, recognition, and detection with commodity mimo-ofdm wifi," *IEEE Internet of Things Journal*, vol. 7, no. 9, pp. 8296–8317, 2020.

[68] D. Zhang, Y. Hu, Y. Chen, and B. Zeng, "Breathtrack: Tracking indoor human breath status via commodity wifi," *IEEE Internet of Things Journal*, vol. 6, no. 2, pp. 3899–3911, 2019.

[69] D. Zhang, Y. He, X. Gong, Y. Hu, Y. Chen, and B. Zeng, "Multitarget aoa estimation using wideband ifmcw signal and two receiver antennas," *IEEE Transactions on Vehicular Technology*, vol. 67, no. 8, pp. 7101–7112, 2018.

[70] Y. He, D. Zhang, Y. Hu, and Y. Chen, "Non-line-of-sight imaging with radio signals," in *2020 Asia-Pacific Signal and Information Processing Association Annual Summit and Conference (APSIPA ASC)*. IEEE, 2020, pp. 11–16.

[71] C. L. Li, M. Liu, and Z. Cao, "Wihf: Gesture and user recognition with wifi," *IEEE Transactions on Mobile Computing*, 2020.

[72] Y. Zou, J. Xiao, J. Han, K. Wu, Y. Li, and L. M. Ni, "Grfid: A device-free rfid-based gesture recognition system," *IEEE Transactions on Mobile Computing*, vol. 16, no. 2, pp. 381–393, 2016.

[73] H. Abdelnasser, K. Harras, and M. Youssef, "A ubiquitous wifi-based fine-grained gesture recognition system," *IEEE Transactions on Mobile Computing*, vol. 18, no. 11, pp. 2474–2487, 2018.

[74] D. Zhang, Y. Hu, Y. Chen, and B. Zeng, "Calibrating phase offsets for commodity wifi," *IEEE Systems Journal*, vol. 14, no. 1, pp. 661–664, 2019.

[75] Q. Xu, Y. Chen, B. Wang, and K. R. Liu, "Trieds: Wireless events detection through the wall," *IEEE Internet of Things Journal*, vol. 4, no. 3, pp. 723–735, 2017.

[76] Y. Han, Y. Chen, B. Wang, and K. R. Liu, "Enabling heterogeneous connectivity in internet of things: A time-reversal approach," *IEEE Internet of Things Journal*, vol. 3, no. 6, pp. 1036–1047, 2016.

[77] Q. Xu, Y. Chen, B. Wang, and K. R. Liu, "Radio biometrics: Human recognition through a wall," *IEEE Transactions on Information Forensics and Security*, vol. 12, no. 5, pp. 1141–1155, 2017.

- [78] Y. Chen, X. Su, Y. Hu, and B. Zeng, “Residual carrier frequency offset estimation and compensation for commodity wifi,” *IEEE Transactions on Mobile Computing*, vol. 19, no. 12, pp. 2891–2902, 2019.
- [79] J. Li, Z. Wang, and X. Hu, “Learning intact features by erasing-inpainting for few-shot classification,” in *Proceedings of the AAAI Conference on Artificial Intelligence*, vol. 35, no. 9, 2021, pp. 8401–8409.
- [80] Y. Li, D. Zhang, J. Chen, J. Wan, D. Zhang, Y. Hu, Q. Sun, and Y. Chen, “Towards domain-independent and real-time gesture recognition using mmwave signal,” *IEEE Transactions on Mobile Computing*, 2022.
- [81] Y. Zou, Z. Yu, X. Liu, B. Kumar, and J. Wang, “Confidence regularized self-training,” in *Proceedings of the IEEE/CVF International Conference on Computer Vision*, 2019, pp. 5982–5991.
- [82] E. Arazo, D. Ortego, P. Albert, N. E. O’Connor, and K. McGuinness, “Pseudo-labeling and confirmation bias in deep semi-supervised learning,” in *2020 International Joint Conference on Neural Networks (IJCNN)*. IEEE, 2020, pp. 1–8.
- [83] H. Bagherinezhad, M. Horton, M. Rastegari, and A. Farhadi, “Label refinery: Improving imagenet classification through label progression,” *arXiv preprint arXiv:1805.02641*, 2018.
- [84] F. C. Robey, D. R. Fuhrmann, E. J. Kelly, and R. Nitzberg, “A cfar adaptive matched filter detector,” *IEEE Transactions on aerospace and electronic systems*, vol. 28, no. 1, pp. 208–216, 1992.